PHYSICAL REVIEW B **82**, 121305(R) (2010)

Cryogenic scanning force microscopy of quantum Hall samples: Adiabatic transport originating in anisotropic depletion at contact interfaces

F. Dahlem,* E. Ahlswede, J. Weis, and K. v. Klitzing
Max-Planck-Institut für Festkörperforschung, Heisenbergstr. 1, D-70569 Stuttgart, Germany
(Received 27 March 2010; revised manuscript received 28 June 2010; published 10 September 2010)

Anisotropic magnetoresistances and intrinsic adiabatic transport features are generated on quantum Hall samples based on an (Al,Ga)As/GaAs heterostructure with alloyed Au/Ge/Ni contacts. We succeed to probe the microscopic origin of these transport features with a cryogenic scanning force microscope by measuring the local potential distribution within the two-dimensional electron system (2DES). These local measurements reveal the presence of an incompressible strip in front of contacts with insulating properties depending on the orientation of the contact/2DES interface line relatively to the crystal axes of the heterostructure. Such an observation gives another microscopic meaning to the term "nonideal contact" used in context with the Landauer-Büttiker formalism applied to the quantum Hall effect.

DOI: 10.1103/PhysRevB.82.121305 PACS number(s): 73.43.−f

Few cryogenic scanning force microscopy (SFM) measurements exist on probing the electrostatic potential distribution in two-dimensional electron systems (2DES) realized in (Al,Ga)As/GaAs heterostructures under quantum Hall conditions.[1,2] Those results measured over the whole 2DES demonstrated the important role of compressible and incompressible strips[3,4] for the current distribution in quantum Hall samples. Despite of these experimental findings, the edge-state picture[5] remains the widely used model to describe the magnetotransport in quantum Hall devices, also in the context of topological insulators.[6] Its success has been partly legitimated by its ability to include contact effects[7] and to explain adiabatic magnetotransport features[8]—such as the disappearance of peaks in the Shubnikov-de Haas (SdH) oscillations, the extension of quantum Hall plateaus to lower magnetic fields, and the existence of nonlocal resistances.[9]

In this Rapid Communication, we manage a comparison between magnetotransport and scanning force microscopy investigations on Hall bar samples showing adiabatic transport features without the use of gates. The SFM measurements present potential distributions from which we conclude that the incompressible strip in front of alloyed contacts possesses different insulating properties depending of the orientation relatively to the crystal axes of the underlying heterostructure. This result shows how to include contacts and interpret adiabatic features in terms of compressible/incompressible strips and what is the microscopic origin of anisotropy in magnetoresistances.

The samples used here are based on an (Al,Ga)As/GaAs heterostructure containing the 2DES at the heterojunction interface 60 nm below the surface. The electron density and mobility at 1.3 K are 3.6×10^{15} m^{-2} and 160 $m^2\,(V\,s)^{-1}$, respectively. Such conditions lead to high electron mobility samples with an electron mean-free path $l\approx13$ μm, which is three times larger than in Ref. 2. Our Hall bars as depicted in Fig. 1 are defined by optical lithography and wet etching. Au/Ge/Ni film is alloyed to achieve low resistive contacts to the 2DES by following our standard recipe.[10] After annealing, the remaining 2DES has a size of about 10 μm width and 58 μm length, which is comparable to the scanning range 20 $\mu m\times20$ μm of our cryogenic SFM. From transmission line measurements, we found an anisotropy in contacting our 2DES in $[01\bar{1}]$ or in [011] crystal direction, which confirms this phenomena as a general property of alloyed Au/Ge/Ni contacts.[10,11] Here the specific resistivity $r_c\equiv R_c\cdot w$ (w, the width of the borderline between 2DES and alloyed metal) is $r_c\approx0.25$ Ω mm for contacts with their borderline perpendicular to [011], and $r_c\approx0.45$ Ω mm for contacts with their borderline perpendicular to $[01\bar{1}]$.

Magnetoresistance $R_{ij,kl}^{[01\bar{1}]}$ in our Hall bar oriented along $[01\bar{1}]$ is obtained with an ac current of 100 nA rms amplitude, which is biased via contacts i and j, and the ac voltage drop between contact k and l is measured by lock-in technique. In comparison to a standard six-terminal Hall bar of same size, these four-terminal Hall bars with two contacts on one side of the mesa display in some magnetoresistances $R_{ij,kl}^{[01\bar{1}]}$ generic adiabatic transport features, reproduced on many samples of same geometry. Examples are given in Fig. 1(a): (1) in measuring the four-terminal longitudinal resistance $R_{14,23}^{[01\bar{1}]}$, resistance peaks of the SdH oscillations are completely suppressed in between $\nu=3$ and 2, and in between $\nu=6$ and 4.[12] (2) The nonlocal resistance $R_{12,34}^{[01\bar{1}]}$ asymmetrically changes with the magnetic field orientation, i.e., for positive magnetic field no voltage drop is observed between contact 3 and 4 ($R_{12,34}^{[01\bar{1}]}=0$) while for negative sign nonzero resistance values are measured. (3) For the two-terminal resistance $R_{14,14}^{[01\bar{1}]}$, Hall plateaus with $R=h/(ie^2)$ are shifted to lower magnetic field values corresponding to filling factors around $\nu=i+1$. We found that Hall plateaus in the two-terminal measurements ($i=k$, $j=l$) are systematically shifted to lower magnetic field values if one of two contacts has its interface line with the 2DES perpendicular to $[01\bar{1}]$ crystal direction. The effect becomes most striking when directly comparing $R_{14,14}$ and $R_{23,23}$ of two Hall bars of same geometry but either oriented along [011] or $[01\bar{1}]$ [see Fig. 1(b)]. The two-terminal Hall resistances $R_{14,14}^{[011]}$ and $R_{23,23}^{[01\bar{1}]}$ superpose whereas $R_{14,14}^{[01\bar{1}]}$ and $R_{23,23}^{[011]}$ deviate.

Until now, all these deviations (1)–(3) in the magnetore-

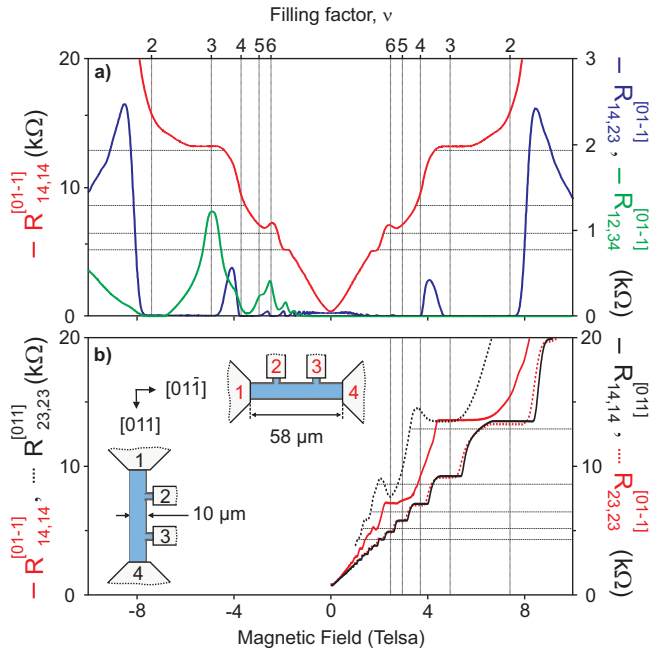

FIG. 1. (Color) Magnetoresistances $R_{ij,kl}$ measured on a four-terminal Hall-bar geometry shown in the inset: (a) Hall plateaus in $R_{14,14}^{[01\bar{1}]}$ (red curve) are shifted to lower magnetic field values, Shubnikov-de Haas peaks in the longitudinal resistance $R_{14,23}^{[01\bar{1}]}$ (blue curve) are missing between $\nu=2-3$, 4–6, and a nonlocal resistance $R_{12,34}^{[01\bar{1}]}$ (green curve) is observed at negative magnetic field ($T=1.3$ K). (b) Comparison of $R_{14,14}$ and $R_{23,23}$ measured on Hall bars oriented either along [011] or [01$\bar{1}$] direction ($T=26$ mK).

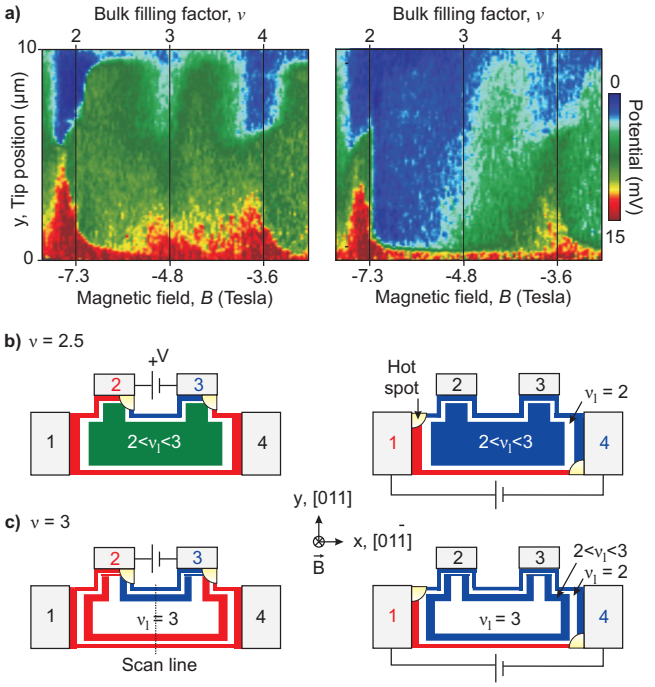

FIG. 2. (Color) (a) Hall potential profiles at negative magnetic fields measured with a cryogenic scanning force microscope. The local potential is recorded along the 10 μm width in the center of the mesa for measurement configurations $R_{23,kl}^{[01\bar{1}]}$ (left) and $R_{14,kl}^{[01\bar{1}]}$ (right). (b) and (c) Sketch of the (incompressible) compressible regions [in (white) color] and potential landscape for $\nu=2.5$ and $\nu=3$, respectively. Further incompressible strips at the edges—if anyhow existing—are suppressed.

sistances have been interpreted in literature within the edge-state picture as a nonequilibrium situation between edge states running along the same edge, caused by full or partial reflection of edge states at imperfect contacts.[8] Here the contacts are however state of the art, i.e., good ohmic and low resistive for both orientations. Furthermore, we demonstrated [see Fig. 1(b)] the control of the intrinsic adiabatic transport features by simply selecting the mesa orientation and its geometry.[13]

In order to investigate the microscopic origins of the previously described adiabatic transport features, we measured the Hall potential distribution within the 2DES. Our scanning force microscope operating at 1.3 K up to 13 T (Ref. 14) is a perfect tool for this purpose. After finding the Hall bar structure at low temperature in a SFM contact mode, the tip is retracted and made oscillating 70 nm above the mesa surface to probe only electrostatic forces. A constant bias voltage is applied between 2DES and metalized cantilever tip compensating for work-function differences and avoiding a gating effect on the 2DES by the tip. As the 2DES is buried in the heterostructure, a special calibration technique[14] has to be used for extracting the Hall potential, i.e., the change in the local electrostatic voltage with current flow through the sample. During a first scan, a $V_m=15$ mV excitation at $w_m=3.4$ Hz is applied to the whole 2DES and the modulation amplitude of the cantilever resonance frequency shift $\Delta f_{res}^{w_m}$ is recorded by lock-in technique along the mesa width. This signal, being proportional to the local excitation, is almost constant with some local variations $M(y)$ due to the donor and surface charges embedded between the 2DES and the cantilever tip: $V^{(1)}(y)=M(y)\cdot V_m$. A second scan is run at the same line with the potential excitation applied only to one contact whereas a second contact is grounded. A 3.4 Hz ac current flows in consequence through the sample and the related Hall potential distribution can be detected by a new $\Delta f_{res}^{w_m}$ measurement: $V^{(2)}(y)=M(y)\cdot V(y)$. The ratio between the second and the first scan $V^{(2)}(y)/V^{(1)}(y)$ delivers the normalized Hall potential profile $V(y)/V_m$ with a spatial lateral resolution better than 100 nm.[14]

In Fig. 2(a), the scanned potential profiles under the condition for measuring $R_{23,kl}^{[01\bar{1}]}$ and $R_{14,kl}^{[01\bar{1}]}$ are presented in a color scale for negative magnetic field (i.e., clockwise rotation of electrons on cyclotron orbits) ranging from below $\nu=2$ to above $\nu=4$. The scans are taken in the middle of the 10-μm-wide mesa as indicated in the Hall bar sketches [Figs. 2(b) and 2(c)]. The colors blue, green, and red in the plots correspond to the lowest, middle, and highest potential value, respectively. For $R_{23,kl}^{[01\bar{1}]}$, the profiles displayed in Fig. 2(a) (left) are similar as obtained in samples with a lower electron mobility of 50 m^2 $(V\ s)^{-1}$ (see Ref. 2). The potential change is rather abrupt near the two edges at the expected positions of the innermost incompressible strips, which merge around $\nu=i$ covering the whole bulk of the 2DES. At this latter filling factor the Hall potential drop is

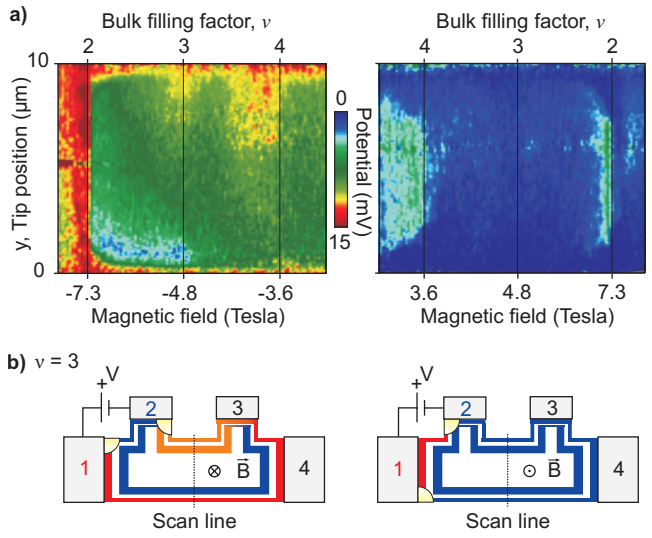

FIG. 3. (Color) (a) Local potential distribution probed for the measurement configuration $R^{[01\bar{1}]}_{12,kl}$. The potential profiles are different in switching the magnetic field orientation. At negative magnetic field in between $2<\nu<3$, a high potential (red) followed by a low potential (blue) is present at one edge. In contrary, the potential stays at low value (blue) for positive magnetic field. (b) Sketch of the (incompressible) compressible regions and potential landscape for $\nu=3$.

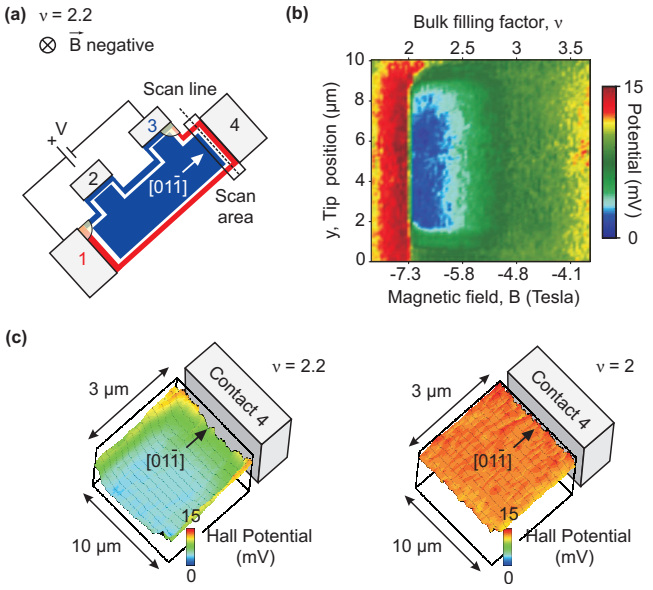

FIG. 4. (Color) (a) Sketch of Hall bar showing our (incompressible) compressible strip model in $R^{[01\bar{1}]}_{13,kl}$ configuration. (b) Corresponding potential distribution for various negative magnetic fields probed on a scan line located at a distance of 1.5 μm from the voltage probing contact 4. (c) x-y potential mapping measured 200 nm away from the contact 4 at $\nu=2.2$ and $\nu=2$. At $\nu=2.2$ the potential remains high (red) along the mesa border whereas the inside has low potential (blue).

then widely spread in the bulk and $R^{[01\bar{1}]}_{23,23}$, shown in Fig. 1(b), behaves normal.

The situation is different for $R^{[01\bar{1}]}_{14,kl}$, where the change in potential happens completely on the lower side of the mesa[15] [see Fig. 2(a)(right)]. This behavior is visible for the whole range between $\nu=2$ and 2.7, and is still strongly pronounced above $\nu=2.7$. In this regime the bulk of the 2DES is compressible with $\nu_l>2$ [in blue color in Fig. 2(b) (right)] and the complete Hall potential drop happens only at the lower mesa side ($y\approx 0$) between this compressible bulk and the compressible edge over the incompressible strip $\nu_l=2$ [white strip in Fig. 2(b) (right)]. The current is thus driven without dissipation within this incompressible strip by the complete Hall voltage V_H, $I=\nu_l e^2/hV_H$.[16] At these filling factors, we can state that there is no equilibration between the compressible bulk with $2<\nu_l<3$ and contacts 1 and 4 [see Fig. 2(b) (right)] as the longitudinal resistance $R^{[01\bar{1}]}_{14,23}$ vanishes for both magnetic field signs in Fig. 1(a). Such a decoupling comes from the depletion regions in front of contacts 1 and 4. These area have smooth electron-density gradient toward the bulk enough to create a wide incompressible strip, which isolates the compressible edge and bulk under high-voltage drops. (For reminder, contacts with such orientation have a higher specific contact resistivity at zero magnetic field.) Turning around the mesa orientation and measuring $R^{[011]}_{14,14}$, the usual transport is recovered [see Fig. 1(b)], i.e., the isolating property of the incompressible strip in front of contacts 1 and 4 with its interface line perpendicular to [011] is not pronounced at $2<\nu<3$. (Such contacts have a lower specific contact resistivity at zero magnetic field.) In Figs. 2(b) and 2(c) the widths of the incompressible strips in front of the contacts are marked smaller or wider in order to indicate their different isolating properties. At lower magnetic field, the two-terminal resistance $R^{[01\bar{1}]}_{14,14}$ shows a Hall plateau with $R=h/(2e^2)$ [see Fig. 1(a)] even at $\nu=3$ where the bulk is mainly incompressible [see Fig. 2(c) (right)]. It follows that the compressible strip with $2<\nu_l<3$ which encircles the incompressible bulk, stays isolated from the compressible edge with $\nu_l<2$ by the incompressible strip $\nu_l=2$. The potential drop is hence located between the two compressible strips at the lower mesa side, a situation which reminds on the adiabatic transport model of nonequilibrium between edge states.

The potential profiles in Fig. 3 correspond to the nonlocal configuration $R^{[01\bar{1}]}_{12,kl}$. For a negative magnetic field between $\nu=2$ and $\nu=3$, the potential drops at the upper mesa side from the edge to the bulk, remains constant over the bulk and drops toward the lower mesa side to increase again at the edge. This unusual potential profile is observed for almost the complete magnetic field range. Obviously, the current driven between contact 1 and 2 runs along the whole edge of the sample passing by contact 3 and 4. Indeed, a nonlocal resistance $R^{[01\bar{1}]}_{12,34}$ has been found for negative magnetic field. For positive fields, no resistance is detected and consistently, the related potential distribution given in Fig. 3(b) shows a constant potential from upper to lower mesa side, i.e., no current passing forth and back through this cross section. As indicated in Fig. 3(b), a decoupling of the bulk and the contacts 1 and 4 is required to explain the presence of nonlocal resistances. Figure 4 presents the x-y potential mapping in the vicinity of contact 4 for the measurement arrangement $R^{[01\bar{1}]}_{13,kl}$. It directly proofs the decoupling by an incompressible

strip at $\nu=2.2$: the potential of the compressible bulk is low even thus the surrounding edge regions on the lower mesa side, in front of the contact 4 and at the upper mesa side are high in potential.

In summary, by comparing magnetotransport and scanning probe investigations, we identified that the presence of an incompressible strip in front of state-of-the-art ohmic contacts might cause an electrical decoupling of the compressible 2DES bulk region from the contacts. Important, we discovered that the insulating properties of this incompressible strip depend on the orientation of the interface line 2DES/alloyed contact relatively to the underlying (Al,Ga)As/GaAs heterostructure. A contact with its interface line perpendicular to [011] equilibrates the compressible bulk and edge, whereas at the same time contacts with the interface line perpendicular to $[01\bar{1}]$ does not. This anisotropy is related to different electron-density profile at the contact interface, which determines in high magnetic field the incompressible strip thickness. Adiabatic transport features hence originates in high electron mobility Hall bar with a geometry having contacts arranged on only three of four sides of the mesa. We conclude, nonideal (ideal) contact behavior in terms of the Landauer-Büttiker formalism can be attributed to a smooth (sharp), partial electrostatic depletion in front of ohmic contacts allowing for an large (thin) isolating incompressible strip.

The authors thank M. Riek and T. Reindl for sample processing help, O. Göktas and Y. Boss for their collaboration in study alloyed contact properties, and A. Siddiki, R. R. Gerhardts, D. Quirion and A. C. Welker for discussions. The 2DES wafer was provided by W. Wegschneider. We acknowledge the Deutsche Forschnungsgemeinschaft (DFG) for financial support under Grant No. WE 1902/1.

*Present address: Néel Institute CNRS/UJF, Grenoble (France); franck.dahlem@grenoble.cnrs.fr

[1] K. L. McCormick, M. T. Woodside, M. Huang, M. Wu, P. L. McEuen, C. Duruoz, and J. S. Harris, Phys. Rev. B **59**, 4654 (1999).

[2] P. Weitz, E. Ahlswede, J. Weis, K. v. Klitzing, and K. Eberl, Physica E **6**, 247 (2000); E. Ahlswede, P. Weitz, J. Weis, K. v. Klitzing, and K. Eberl, Physica B **298**, 562 (2001); Physica E **12**, 165 (2002).

[3] D. B. Chklovskii, B. I. Shklovskii, and L. I. Glazman, Phys. Rev. B **46**, 4026 (1992).

[4] A. Siddiki and R. R. Gerhardts, Phys. Rev. B **68**, 125315 (2003); D. Eksi, O. Kilicoglu, O. Goektas, and A. Siddiki, arXiv:1003.5963 (unpublished); A. Siddiki and R. R. Gerhardts, Phys. Rev. B **70**, 195335 (2004); K. Lier and R. R. Gerhardts, *ibid.* **50**, 7757 (1994).

[5] M. Büttiker, Phys. Rev. B **38**, 9375 (1988).

[6] A. Roth, C. Brüne, H. Buhmann, L. Molenkamp, J. Maciejko, X. Qi, and S. Zhang, Science **325**, 294 (2009); M. Büttiker, *ibid.* **325**, 278 (2009).

[7] In controlled experiments, "ideal and nonideal" contact properties are mimicked by locally depleting the 2DES by gate electrodes in front of contacts.

[8] R. Haug, Semicond. Sci. Technol. **8**, 131 (1993); C. W. J. Beenakker and H. van Houten, Solid State Phys. **44**, 1 (1991).

[9] S. Komiyama and H. Nii, Physica B **184**, 7 (1993); B. W. Alphenaar, P. L. McEuen, R. G. Wheeler, and R. N. Sacks, Phys. Rev. Lett. **64**, 677 (1990); P. L. McEuen, A. Szafer, C. A. Richter, B. W. Alphenaar, J. K. Jain, A. D. Stone, R. G. Wheeler, and R. N. Sacks, *ibid.* **64**, 2062 (1990); B. J. van Wees, E. M. M. Willems, L. P. Kouwenhoven, C. J. P. M. Harmans, J. G. Williamson, C. T. Foxon, and J. J. Harris, Phys. Rev. B **39**, 8066 (1989).

[10] O. Göktas, J. Weber, J. Weis, and K. v. Klitzing, Physica E **40**, 1579 (2008).

[11] M. Kamada, T. Suzuki, F. Nakamura, Y. Mori, and M. Arai, Appl. Phys. Lett. **49**, 1263 (1986).

[12] The filling factor is obtained from the electron density n_s and magnetic field B by $\nu=2\pi\hbar n_s/(eB)$.

[13] C. Uiberacker, C. Stecher, and J. Oswald, Phys. Rev. B **80**, 235331 (2009).

[14] P. Weitz, E. Ahlswede, J. Weis, K. v. Klitzing, and K. Eberl, Appl. Surf. Sci. **157**, 349 (2000).

[15] A similar profile was observed on a gated Hall bar by M. Woodside, C. Valea, K. McCormick, P. McEuen, C. Kadow, K. D. Maranowski, and A. C. Gossard, Physica E **6**, 238 (2000).

[16] The current is hence concentrated in a region of carrier density smaller than the bulk density as it was expected from the shift of Hall plateaus to lower magnetic fields.